Synthesis, Structure, and Physical Properties of Nickel Bis(dithiolene) Metal Complexes, [Ni(dmit)$_2$], with Highly Polar Cyanine Dyes

Isabelle Malfant, Raquel Andreu, Pascal G. Lacroix,* Christophe Faulmann, and Patrick Cassoux

Equipe Précurseurs Moléculaires et Matériaux, LCC/CNRS, 205 Route de Narbonne, 31077 Toulouse Cedex, France

Received December 10, 1997

Three new compounds were obtained by slow diffusion of $[Ni(dmit)_2]^-$ (dmit = 2-thioxo-1,3-dithiole-4,5-dithiolato) into 4-(dimethylamino)-1-methylpyridinium $[C_1]^+$, 4-[2-(4-(dimethylamino)phenyl)ethenyl]-1-methylpyridinium $[C_2]^+$, and 4-[4-(4-(dimethylamino)phenyl)-1,3-butadienyl]-1-methylpyridinium $[C_3]^+$. $[C_1]^+[Ni(dmit)_2]^-$ exhibits two crystallographic phases (**1**, **2**) as does $[C_2]^+[Ni(dmit)_2]^-$ (**3**, **4**). The structures have been determined: **1**, monoclinic, $P2_1/c$, $a = 17.450(2)$ Å, $b = 10.646(1)$ Å, $c = 23.891(2)$ Å, $\beta = 97.42(1)°$, $Z = 4$; **2**, triclinic $P\bar{1}$, $a = 9.776(1)$ Å, $b = 15.195(2)$ Å, $c = 16.999(2)$ Å, $\alpha = 114.14(1)°$, $\beta = 101.84(1)°$, $\gamma = 93.40(1)°$, $Z = 2$; **3**, monoclinic, $P2_1/c$, $a = 9.813(1)$ Å, $b = 11.589(1)$ Å, $c = 24.345(3)$ Å, $\beta = 93.12(1)°$, $Z = 4$; **4**, triclinic, $P\bar{1}$, $a = 13.432(2)$ Å, $b = 16.101(2)$ Å, $c = 6.553(1)$ Å, $\alpha = 99.69(1)°$, $\beta = 94.34(1)°$, $\gamma = 102.88(2)°$, $Z = 2$; $[C_1]^+[Ni(dmit)_2]^-$ (**1**) exhibits a conductivity of 1.3×10^{-2} S cm^{-1}. Due to centrosymmetry, none of the materials exhibits second-order nonlinear optical properties, but the structure of **1** demonstrates that layers of highly polarizable cations can be stabilized in a noncentrosymmetric environment between two-dimensional networks of $[Ni(dmit)_2]^-$ species.

Introduction

The rapid developments in the field of telecommunications and computing devices are pressing the need for improved electronic components. The emerging technology of photonics, which uses nonlinear optical (NLO) materials for high-speed digital switching and frequency conversion, has been labeled the technology of the twentyfirst century.[1,2] In any case, the possible shift from electronics to photonics will probably be gradual, and during the transition period, the hybrid technology of optoelectronics, in which electrons interface with photons, will become increasingly important. Molecular chemistry offers a unique opportunity to design materials combining several properties (e.g. magnetism and conductivity,[3,4] or magnetism and nonlinear optics[5]) that could hopefully be coupled in an actual interplay. Following this idea, linking conductivity and NLO properties would also provide the interest to associate semiconductor-based electronics and NLO-based photonics within a research effort aiming at connecting these technologies.

The past few years have seen the emergence of a new class of polymeric materials exhibiting photorefractivity, a property that combines photoconductivity and electrooptic response,[6] but very little has been published on molecular materials.[7−9] We have recently reported on a family of derivatives combining efficient second-order NLO chromophores and 7,7′,8,8′-tetracyanoquinodimethane [tcnq] acceptors, a counterion that could bring about NLO materials with conducting properties.[9] The absence of crystal structures did not allow the full understanding of the origin and extent of the possibly coupled properties. Following a similar strategy, [Ni(dmit)$_2$]-based systems ($dmit^{2-}$ = 2-thioxo-1,3-dithiole-4,5-dithiolato; Chart 1), instead of [tcnq], could be used as a component awarding conducting properties to the desired hybrid compound. Nickel bis(dithiolene) derivatives such as [Ni(dmit)$_2$] have received considerable attention since the discovery of superconductivity in $[ttf][Ni(dmit)_2]_2$,[10] a property that has never been observed in any [tcnq]-based materials. Combining [Ni(dmit)$_2$]-based anions with cationic chromophores may lead to the preparation of molecular systems exhibiting both NLO and conducting properties. Among possible candidate cations, we have selected the highly polarizable "push−pull" cyanines, 4-(dimethylamino)-1-methylpyridinium $[C_1]^+$, 4-[2-(4-(dimethylamino)phenyl)ethenyl]-1-methylpyridinium $[C_2]^+$, and 4-[4-(4-(dimethylamino)phenyl)-1,3-butadienyl]-1-methylpyridinium $[C_3]^+$ (Chart 1).

Experimental Section

Starting Materials and Equipment. Acetonitrile was purchased from SDS and distillated over P_2O_5 prior to use. $(n\text{-}Bu_4N)[Ni(dmit)_2]$,[11]

(1) Dalton, L. R.; Harper, A. W.; Ghosn, R.; Steier, W. H.; Ziari, M.; Fetterman, H.; Shi, Y.; Mustacich, R. V.; Jen A. K. Y.; Shea, K. J. *Chem. Mater.* **1995**, *7*, 1060.
(2) Dagani, R. *Chem. Eng. News* **1996**, *March 4*, 22.
(3) Goze, F.; Laukhin, V. N.; Brossard, L.; Audouard, A.; Ulmet, J. P.; Askenazy, S.; Naito, T.; Kobayashi, H.; Kobayashi M.; Cassoux, P. *Europhys. Lett.* **1994**, *28*, 427.
(4) Kurmoo, M.; Graham, A. W.; Day, P.; Coles, S. J.; Hursthouse, M. B.; Caulfield, J. L.; Singleton, J.; Pratt, F. L.; Hayes, W.; Ducasse L.; Guionneau, P. *J. Am. Chem. Soc.* **1995**, *117*, 12209.
(5) (a) Clément, R.; Lacroix, P. G.; O'Hare D.; Evans, J. *Adv. Mater.* **1994**, *6*, 794. (b) Lacroix, P. G.; Clément, R.; Nakatani, K.; Zyss J.; Ledoux, I. *Science* **1994**, *263*, 658.
(6) Yu, L.; Chan, W. K.; Peng Z.; Gharavi, A. *Acc. Chem. Res.* **1996**, *29*, 13.
(7) Sutter, K.; Hulliger J.; Günter, P. *Solid State Commun.* **1990**, *74*, 867.
(8) (a) Shan, B. Z.; Zhang, X. M.; You, X. Z.; Fun H. K.; Sivakumar, K. *Acta Cryst.* **1996**, *C52*, 1148. (b) Fun, H. K.; Sivakumar, K.; Shan B. Z.; You, X. Z. *Acta Crystallogr.* **1996**, *C52*, 1152.
(9) Lacroix P. G.; Nakatani, *Adv. Mater.* **1997**, *9*, 1105.
(10) (a) Brossard, L.; Ribault, M.; Valade L.; Cassoux, P. *Phys. B* **1986**, *143*, 378. (b) Cassoux, P.; Valade, L.; Kobayashi, H.; Kobayashi, A.; Clark, R. A.; Underhill, A. *Coord. Chem. Rev.*, **1991**, *110*, 115. (c) Cassoux P.; Valade, L. In *Inorganic Materials*; Bruce D. W., O'Hare, D., Eds.; Wiley: Chichester, 1992; pp 1−58.

S0020-1669(97)01550-4 CCC: $15.00
Published on Web 06/06/1998

Chart 1

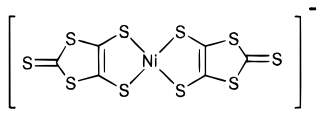

$[Ni(dmit)_2]^-$

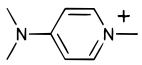

C_1^+

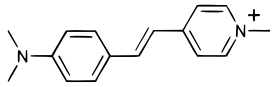

C_2^+

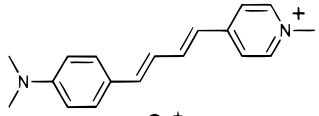

C_3^+

4-(dimethylamino)-1-methylpyridinium $[C_1]^+$,[12] 4-[2-(4-(dimethylamino)phenyl)ethenyl]-1-methylpyridinium $[C_2]^+$,[13] and 4-[4-(4-(dimethylamino)phenyl)-1,3-butadienyl]-1-methylpyridinium $[C_3]^+$,[14,15] were synthesized as previously described. Elemental analyses were performed by the "Service de Microanalyses du Laboratoire de Chimie de Coordination" in Toulouse, France.

Synthesis. Crystals were obtained by slow interdiffusion of saturated solution of $(n\text{-}Bu_4N)[Ni(dmit)_2]$ and $[C_1]^+I^-$ or $[C_2]^+I^-$. These experiments were carried out under argon, in a three-compartment H-tube equipped with porous glass frits between the compartments. The concentrations of the solutions were kept close to saturation during the diffusion process by means of additional porous containers placed in the appropriate compartment and filled with an excess of solid starting reagents. Attempts to grow crystals from $[C_3]^+I^-$ were unsuccessful and, therefore, $[C_3][Ni(dmit)_2]$ has been obtained as powder samples only. Anal. Calcd for $C_{22}H_{21}N_2NiS_{10}$: C, 40.22; H, 2.95; N, 3.91. Found: C, 41.7; H, 2.6; N, 4.0.

Structure Analysis and Refinement. The structures were solved by direct methods (SHELXS86)[16] and refined by least-squares procedures. Crystallographic data for $[C_1][Ni(dmit)_2]$ and $[C_2][Ni(dmit)_2]$ are summarized in Table 1. The calculations were carried out with the CRYSTALS package programs[17] running on a PC. The drawings of the molecular structures were obtained with the help of CAMERON.[17] The atomic scattering factors were taken from *International Tables for X-ray Crystallography*.[18] Full X-ray data, fractional atomic coordinates, and the equivalent thermal parameters for all atoms and anisotropic thermal parameters have been deposited at the Cambridge Crystallographic Data Center.

Electronic Band Structure Calculations. The electronic structures were obtained on the basis of extended Hückel[19] tight-binding (EHTB) band structure calculations.[20] The off-diagonal matrix elements of the effective Hamiltonian were calculated according to the modified Wolfsberg−Helmholz formula. The exponents, contraction coefficients, and atomic parameters used in the calculations are tabulated as previously reported.[21]

Conductivity. Temperature-dependent single-crystal conductivity measurements were carried out following the standard four-probe technique. Electrical contacts were obtained by gluing four gold wires to the crystal with Emetron M8001 gold paint. The sample mounted on a Motorola printed circuit was placed in an Oxford Instruments model CF 200 continuous-flow cryostat. Temperature control and temperature-resistance data acquisition were achieved using an Oxford Instruments model DTC2 PID temperature controller, and a Hewlett-Packard model 4263A LCR meter, respectively, both driven by a personal computer running in-house software. Powder conductivity measurements were carried out on pressed pellets of pure powder materials (size: 1 mm^2 × about 1 mm) obtained by careful grinding. The cylinders used to press the materials were used as electrodes.

Results and Discussion

Synthesis. Every material presented in this study is obtained by slow diffusion of $[Ni(dmit)_2]^-$ anions through a solution containing the appropriate $[C]^+$ countercation. Contrary to what was reported in our previous paper based on $TCNQ^0/TCNQ^-$ mixed-valence species, the highly unsoluble neutral $[Ni(dmit)_2]$ compound is not a convenient starting material. The syntheses have to be carried out with $[Ni(dmit)_2]^-$ as the only nickel-containing species allowed to react with $[C]^+$. After 2 months of slow diffusion, two types of single crystals were obtained with $[C_1]^+$: black elongated plates designated hereafter as phase **1**, and diamond-shaped dark solid designated hereafter as phase **2**. Both phases have been characterized by X-ray diffraction studies (see below) as having the same 1:1 $[C_1][Ni(dmit)_2]$ stoichiometry. Likewise, two types of single crystals were obtained with $[C_2]^+$, as thick plates and square plates labeled hereafter phase **3** and **4** respectively, and having the same 1:1 $[C_2][Ni(dmit)_2]$ stoichiometry, as shown by X-ray studies.

Description of Structures. $[C_1][Ni(dmit)_2]$ (Phase 1). The asymmetric unit is shown in Figure 1 with the atomic numbering scheme used. It consists of two planar $[Ni(dmit)_2]$ entities labeled **A** and **B**, (largest deviations from planarity are 0.106 Å for S(5) in **A** and 0.072 for S(15) in **B**) and two $[C_1]^+$ cations. No atoms are in special positions. A collection of some relevant intramolecular distances is given in Table 2 for the $[Ni(dmit)_2]$ species. The mean Ni−S distances are 2.165(1) and 2.164(1) Å for molecules **A** and **B**, respectively, which is somewhat larger than those observed for other compounds of general formula $[Cat]^+[Ni(dmit)_2]^-$ were $[Cat]^+$ is a closed-shell cation. For comparison, the Ni−S distances observed for $[Cat]^+ = [NMe_4]^+$, $[NEt_4]^+$, $[NPr_4]^+$, and $[NBu_4]^+$ are 2.158(3),[22] 2.157(4),[23] 2.160(3),[22] and 2.156[24] Å, respectively. However, this result is in agreement with the situation encountered in $[C_6H_{11}N_2]^+$-

(11) (a) Steimecke, G.; Sieler, H. J.; Kirmse R.; Hoyer, E. *Phosphorous Sulfur* **1979**, *7*, 49. (b) Valade, L.; Legros, J. P.; Bousseau, M.; Cassoux, P.; Garbauskas M.; Interrante, L. *J. Chem. Soc., Dalton Trans.* **1985**, 783.
(12) Rollema, H.; Johnson, E. A.; Booth, R. G.; Caldera, P.; Lampen, P.; Youngster, S. K.; Trevor, A. J.; Naiman N.; Castagnoli, N. *J. Med. Chem.* **1990**, *33*, 2221.
(13) Kung, T. K. *J. Chin. Chem. Soc.* **1978**, *25*, 131.
(14) Duan, X. M.; Okada, S.; Oikawa, H.; Matsuda H.; Nakanishi, H. *Mol. Cryst. Liq. Cryst.* **1995**, *267*, 89.
(15) Matsui, M.; Kawamura, S.; Shibata, K.; Muramatsu, H. *Bull. Chem. Soc. Jpn.* **1992**, *65*, 71.
(16) Sheldrick G. M. *SHELXS86: Program for Crystal Structure Solution*; University of Göttingen: Göttingen, Germany, 1986.
(17) (a) Watkin, D. J.; Prout, C. K.; Carruthers, J. R.; Betteridge, P. W. *CRYSTALS*, Issue 10; Chemical Crystallography Laboratory, University of Oxford: Oxford, England, 1996. (b) Watkin, D. J.; Prout, C. K.; Pearce, L. J. *CAMERON*; Chemical Crystallography Laboratory, University of Oxford: Oxford, England, 1996.
(18) Cromer, D. T.; Waber, J. T. *International Tables for X-ray Crystallography*; Kynoch Press: Birmingham, 1974; Vol. 4.
(19) (a) Hoffmann, R. *J. Chem. Phys.* **1963**, *39*, 1397. (b) Ammeter, J. H.; B.; Bürgi, H. B.; Thibeault, J.; Hoffmann, R. *J. Am. Chem. Soc.* **1978**, *100*, 3686.
(20) Whangbo, M.-H.; Hoffman, R. *J. Am. Chem. Soc.* **1978**, *100*, 6093.
(21) Canadell, E.; Rachidi, I. E.-I.; Ravy, S.; Pouget, J. P.; Brossard, L.; Legros, J. P., *J. Phys. France* **1989**, *50*, 2967.
(22) van Diemen, J. H.; Groeneveld, L. R.; Lind, A.; de Graaff, R. A. G.; Haasnoot, J. G.; Reedijk, J. *Acta Crystallogr.* **1988**, *C44*, 1898.
(23) Groeneveld, L. R.; Schuller, B.; Kramer, G. J.; Haasnoot, J. G.; Reedijk, J. *Recl. Trav. Chim. Pays-Bas* **1986**, *105*, 507.
(24) Lindqvist, O.; Andersen, L.; Sieler, H. J.; Steimecke, G.; Hoyer, E. *Acta Chem. Scand.* **1982**, *A36*, 855.

Table 1. Crystal Data for $[C_1][Ni(dmit)_2]$ (Phases **1** and **2**) and $[C_2][Ni(dmit)_2]$ (Phases **3** and **4**)

	1	**2**	**3**	**4**
crystal data				
formula	$C_{28}H_{26}N_4Ni_2S_{20}$	$C_{28}H_{26}N_4Ni_2S_{20}$	$C_{22}H_{19}N_2NiS_{10}$	$C_{22}H_{19}N_2NiS_{10}$
M (g mol^{-1})	1177.2	1177.2	690.7	690.7
crystal shape	elongated plates	diamond shapes	thick plates	squared plates
color	black	black	black	black
size (mm)	0.75 × 0.1 × 0.05	0.57 × 0.5 × 0.12	0.3 × 0.425 × 0.04	0.52 × 0.15 × 0.07
crystal system	monoclinic	triclinic	monoclinic	triclinic
space group	$P2_1/c$	$P\bar{1}$	$P2_1/c$	$P\bar{1}$
a (Å)	17.450(2)	9.776(1)	9.813(1)	13.432(2)
b (Å)	10.646(1)	15.195(2)	11.589(1)	16.101(2)
c (Å)	23.891(2)	16.999(2)	24.345(3)	6.553(1)
α (°)		114.14(1)		99.69(1)
β (°)	97.42(1)	101.84(1)	93.12(1)	94.34(1)
γ (°)		93.40(1)		102.88(2)
U (Å^3)	4401.1	2226.1	2765	1347
Z	4	2	4	2
D_c	1.776	1.756	1.66	1.70
F(000)	2403.1	1201.5	1417.6	708.8
data collection				
diffractometer	IPDS Stoe	IPDS Stoe	IPDS Stoe	Enraf-Nonius CAD4
monochromator	graphite	graphite	graphite	graphite
μ(Mo Kα) (cm^{-1})	18.0	17.8	14.5	14.8
temperature (K)	160	293	293	293
scan mode	ϕ	ϕ	ϕ	$\omega/2\theta$
scan range ϕ (deg)	$0 < \phi < 200$	$0 < \phi < 250.5$	$0 < \phi < 200.2$	$0.80 + 0.35 \tan\theta$
2θ range (deg)	$2.9 \le 2\theta \le 48.4$	$2.9 \le 2\theta \le 48.4$	$2.9 \le 2\theta \le 48.4$	$\theta_{max} = 25°$
absorption correction	none	none	none	none
no. of reflcns collcd	28 505	17 675	16 184	5205
no. of indep reflcns	6928	6533	4164	4752
no. of indep obsd reflcns	4836 [$I > 0.5\sigma(I)$]	5305 [$I > 2\sigma(I)$]	2311 [$I > 3\sigma(I)$]	2947 [$I > 3\sigma(I)$]
range of h, k, l	$-15 \le h \le 15$	$-11 \le h \le 10$	$-11 \le h \le 11$	$-16 \le h \le 16$
	$0 \le k \le 12$	$-17 \le k \le 15$	$0 \le k \le 13$	$-19 \le k \le 19$
	$0 \le l \le 27$	$0 \le l \le 19$	$0 \le l \le 27$	$0 \le l \le 7$
variation in standards (%)	not significant	not significant	not significant	not significant
refinement				
refinement on	F	F	F	F
R[a]	0.0480	0.0382	0.0253	0.0255
wR[b]	0.0408	0.0458	0.0256	0.0289
no. of reflections used				
no. of reflcns used in refinement	4836	5305	2311	2947
no. of variables	488	520	391	391
H-atom treatment	calculated	calculated for CH_3 otherwise refined isotropically	refined isotropically	refined isotropically
weighting scheme	Chebychev	Chebychev	Chebychev	Chebychev
coeff. Ar	1.676	1.101	1.557	3.608
	1.687	0.823	0.475	−3.116
	1.829	0.711	1.822	2.744
	0.680		0.180	−1.079
	0.507		0.536	
$(\Delta/\sigma)_{max}$	0.04	0.06	0.09	0.03
$\Delta\rho_{max}$ (e Å^{-3})	0.61	0.41	0.34	0.40
$\Delta\rho_{min}$ (e Å^{-3})	−0.81	−0.57	−0.24	−0.21
GOF	1.09	1.00	1.11	1.14

[a] $R = \sum(||F_o| - |F_c||)/\sum(|F_o|)$. [b] $wR = \sum w(|F_o| - |F_c|)^2/\sum w(F_o)^2]^{1/2}$.

$[Ni(dmit)_2]^-$ reported by Reedijk et al.[25] According to these authors, the overall electronic structure of $[Ni(dmit)_2]$ may be slightly modified through possible π-overlap of the orbital of the cations with those of the anions, but is still very far from the 2.216(6) Å reported for $[Ni(dmit)_2]^{2-}$ derivatives.[26] In conclusion, the charge of $[Ni(dmit)_2]$ is undoubtedly −1.

A projection of the structure of **1** onto the *bc* plane is shown in Figure 2. The structure is made up of layers of $[Ni(dmit)_2]^-$ anions separated by layers of $[C_1]^+$ cations. The angle between the mean planes of two independent $[Ni(dmit)_2]^-$ anions with short S···S contacts (**A** and **B**) is 10.19°. The intralayer distance is equal to 5.209 Å. A projection of the anions onto the *ac* plane (Figure 3) reveals that the $[Ni(dmit)_2]^-$ units are organized in a two dimensionnal network of molecules connected through short S···S van der Waals contacts (<3.7 Å). Three short S···S distances between neighboring molecules are observed along the [001] direction versus only one along the [100] direction, the latter one involving the external thione groups. The lengths of S···S contacts are gathered in Table 3. Between the $[Ni(dmit)_2]^-$ planes, layers of $[C_1]^+$ cations are inserted, their molecular planes roughly parallel to the $[Ni(dmit)_2]^-$ layers. A projection onto the *ac* plane is shown in Figure 4. It reveals that although phase **1** is centrosymmetric (space group $P2_1/c$), the $[C_1]^+$ cations are engineered in a noncentrosymmetric

(25) Reefman, D.; Cornelissen, J. P.; Haasnoot, J. G.; de Graaff, R. A. G.; Reedijk, J. *Inorg. Chem.* **1990**, *29*, 3933.
(26) Lindqvist, O.; Sjölin, L.; Sieler, J.; Steimecke, G.; Hoyer, E. *Acta Chem. Scand.* **1979**, *A33*, 445.

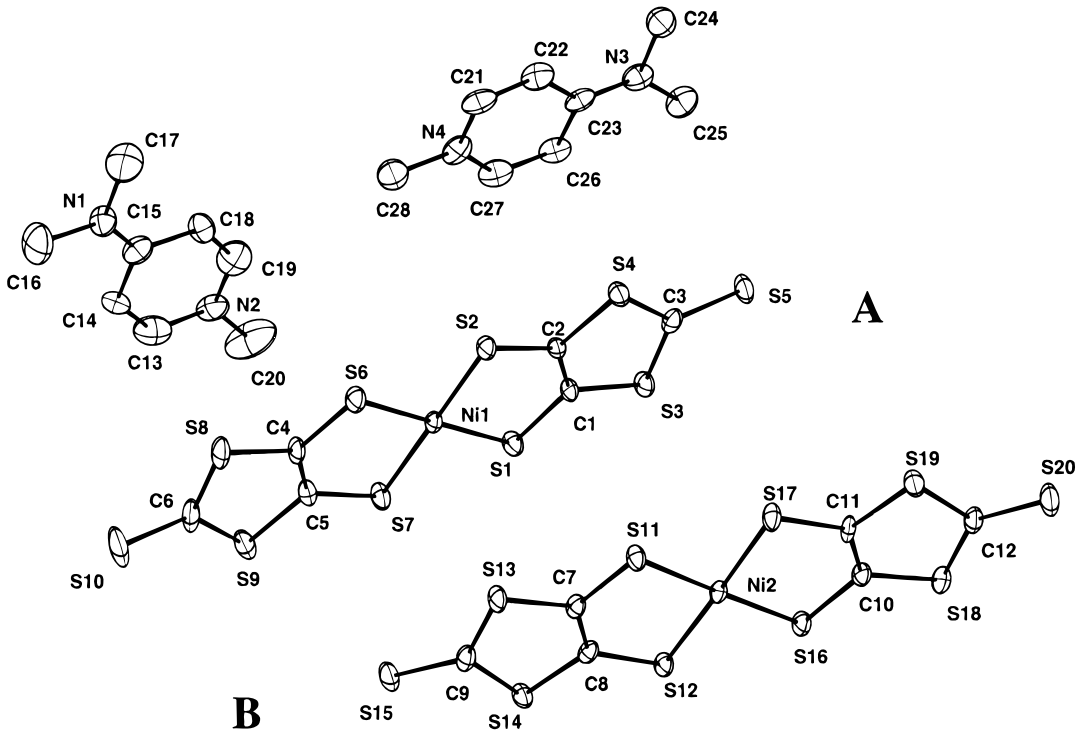

Figure 1. Asymmetric unit and atomic labeling system for $[C_1][Ni(dmit)_2]$ (phase **1**). H atoms are omitted for clarity.

Table 2. Selected Bond Lengths (Å) for $[C_1][Ni(dmit)_2]$ (Phases **1** and **2**) and for $[C_2][Ni(dmit)_2]$ (Phases **3** and **4**) (**A** and **B** Refer to the Two Nonequivalent $[Ni(dmit)_2]^-$ Present in Phases **1** and **2**)

phase **1**				phase **2**				compound $[C_2][Ni(dmit)_2]$			
molecule **A**		molecule **B**		molecule **A**		molecule **B**		phase **3**		phase **4**	
Ni(1)−S(1)	2.163(1)	Ni(2)−S(11)	2.163(1)	Ni(1)−S(1)	2.1648(8)	Ni(2)−S(11)	2.1584(9)	Ni(1)−S(1)	2.167(1)	Ni(1)−S(1)	2.1634(8)
Ni(1)−S(2)	2.162(1)	Ni(2)−S(12)	2.166(1)	Ni(1)−S(2)	2.1639(8)	Ni(2)−S(12)	2.1740(8)	Ni(1)−S(2)	2.154(1)	Ni(1)−S(2)	2.1709(8)
Ni(1)−S(6)	2.165(1)	Ni(2)−S(16)	2.164(1)	Ni(1)−S(6)	2.1684(8)	Ni(2)−S(16)	2.1822(9)	Ni(1)−S(6)	2.161(1)	Ni(1)−S(6)	2.1579(8)
Ni(1)−S(7)	2.169(1)	Ni(2)−S(17)	2.164(1)	Ni(1)−S(7)	2.1650(8)	Ni(2)−S(17)	2.1631(8)	Ni(1)−S(7)	2.156(1)	Ni(1)−S(7)	2.1663(8)
S(1)−C(1)	1.713(5)	S(11)−C(7)	1.730(5)	S(1)−C(1)	1.716(3)	S(11)−C(7)	1.707(3)	S(1)−C(1)	1.717(4)	S(1)−C(1)	1.709(3)
S(2)−C(2)	1.695(5)	S(12)−C(8)	1.715(5)	S(2)−C(2)	1.711(3)	S(12)−C(8)	1.720(3)	S(2)−C(2)	1.710(4)	S(2)−C(2)	1.720(3)
S(6)−C(4)	1.720(5)	S(16)−C(10)	1.727(5)	S(6)−C(4)	1.718(3)	S(16)−C(10)	1.723(3)	S(6)−C(4)	1.703(4)	S(6)−C(4)	1.699(3)
S(7)−C(5)	1.728(5)	S(17)−C(11)	1.719(4)	S(7)−C(5)	1.714(3)	S(17)−C(11)	1.717(3)	S(7)−C(5)	1.699(4)	S(7)−C(5)	1.710(3)

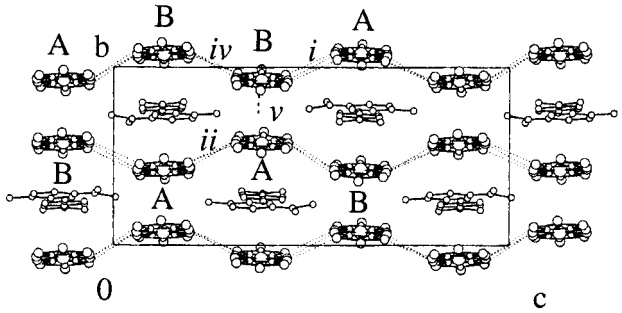

Figure 2. Projection of the $[C_1][Ni(dmit)_2]$ unit of phase **1** onto the *bc* plane.

environment between the layers of anions. The angle between the two longitudinal nitrogen−nitrogen axis of the cations is equal to 115.07°.

$[C_1][Ni(dmit)_2]$ (Phase 2). The asymmetric unit contains two planar $[Ni(dmit)_2]$ entities labeled **A** and **B** (largest deviations are 0.135 Å for S(15) in **A** and 0.092 for S(20) in **B**) and two $[C_1]^+$ cations, with the same atom labeling as in phase **1**. A collection of some relevant intramolecular distances in the $[Ni(dmit)_2]^-$ species is given in Table 2. The mean Ni−S distances are 2.166(1) and 2.169(1) Å for molecules **A** and **B**, respectively, which is very similar to what is observed in phase

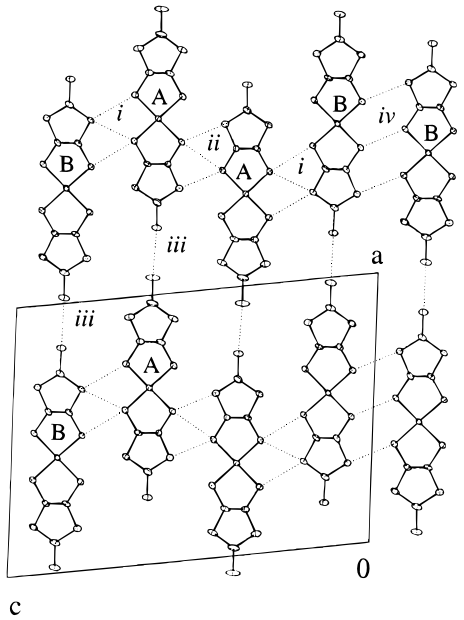

Figure 3. Projection of the $[Ni(dmit)_2]$ layers onto the *ac* plane for $[C_1][Ni(C_3S_5)_2]$ (phase **1**). The dotted lines represent the S···S distances shorter than the sum (3.7 Å) of the van der Waals radii.

Table 3. S···S Intermolecular Contacts (<3.7 in Å) for $[C_1][Ni(dmit)_2]$ (Phases **1** and **2**) and $[C_2][Ni(dmit)_2]$ (Phases **3** and **4**)

phase **1**		phase **2**		phase **3**		phase **4**	
atoms[a]	distances	atoms[b]	distances	atoms[c]	distances	atoms[d]	distances
S(1)−S(11i)	3.648 (2)	S(2)−S(13i)	3.573 (1)	S(2)−S(2i)	3.667 (2)	S(1)−S(2i)	3.663 (1)
S(1)−S(13i)	3.418 (2)	S(6)−S(13i)	3.539 (1)	S(2)−S(4i)	3.496 (1)	S(1)−S(6i)	3.491 (1)
S(7)−S(13i)	3.513 (2)	S(7)−S(9ii)	3.490 (1)	S(4)−S(10ii)	3.662 (2)	S(7)−S(6i)	3.661 (1)
S(2)−S(2ii)	3.645 (2)	S(5)−S(10iii)	3.469 (1)			S(3)−S(2i)	3.618 (1)
S(2)−S(4ii)	3.635 (2)	S(15)−S(20iii)	3.597 (1)			S(7)−S(8i)	3.602 (1)
S(5)−S(10iii)	3.489 (2)	S(12)−(14iv)	3.509 (1)			S(1)−S(7ii)	3.699 (1)
S(20)−S(15iii)	3.475 (2)					S(4)−S(5iv)	3.608 (1)
S(12)−S(12iv)	3.490 (2)					S(5)−S(5v)	3.670 (2)
S(14)−S(16iv)	3.539 (2)						

[a] Symmetry operations for second atom: (i) x, y, z; (ii) $1-x, 1-y, 1-z$; (iii) $1+x, y, z$; (iv) $1-x, 1-y, -z$. [b] Symmetry operations for second atom: (i) x, y, z; (ii) $-x, -y, 1-z$; (iii) $x+1, y+1, z$; (iv) $2-x, -y, 2-z$. [c] Symmetry operations for second atom: (i) $1-x, -y, 1-z$; (ii) $-x, -y, 1-z$. [d] Symmetry operations for second atom: (i) $x, y, z-1$; (ii) $2-x, 2-y, -z$; (iii) $1-x, 1-y, -z$; (iv) $1-x, 1-y, -1-z$.

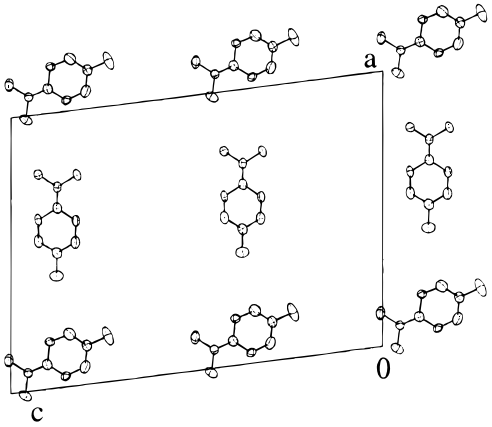

Figure 4. Projection of $[C_1]^+$ layers onto the *ac* plane for $[C_1][Ni(dmit)_2]$ (phase **1**) showing the acentric environment of the chromophores. H atoms are omitted for clarity.

1. Consequently, a −1 charge can be assigned for $[Ni(dmit)_2]$ species in this compound.

At first, the overall structure of phase **2** seems to be very closely related to that of phase **1**. It consists on layers of overlapping $[Ni(dmit)_2]^-$ anions in the $(\bar{1}12)$ plane, separated by layers of $[C_1]^+$ cations. The angle between the mean planes of the two independent $[Ni(dmit)_2]^-$ anions (**A** and **B**) is 3.06°. The interlayer distance is equal to 5.603 Å versus 5.209 Å for phase **1**. A projection of the anions onto the $(\bar{1}12)$ plane (Figure 5) reveals that the $[Ni(dmit)_2]^-$ units are organized in a two dimensionnal network through short S···S van der Waals contacts (<3.7 Å). A careful comparison of Figures 3 and 5 reveals an important difference between phases **1** and **2**, mainly involving the orientation of the **B** $[Ni(dmit)_2]^-$ units in the cell. These anions are slightly shifted apart from one another along the [110] direction in phase **2** and along the $[\bar{1}12]$ direction (perpendicular to the mean plane of the $[Ni(dmit)_2]^-$ layer), the distance between their molecular planes reaching 1.817 Å versus 1.598 Å in phase **1**. Consequently, the S···S short contacts are modified, with a loss of one-third of the short S···S contacts along the [201] direction. Compared to phase **1**, another major difference is observed in phase **2**. A layer of $[C_1]^+$ cations is shown in Figure 6. Contrary to the situation encountered in phase **1**, the cations are engineered in a centrosymmetric environment within their layers in phase **2**.

$[C_2][Ni(dmit)_2]$ (Phase 3). The asymmetric unit with the atomic numbering scheme is shown in Figure 7. Intramolecular distances are in agreement with those found in the previous compound $[C_1][Ni(dmit)_2]$. Therefore, as for phases **1** and **2**, the −1 charge can be assigned to the $[Ni(dmit)_2]$ unit. The

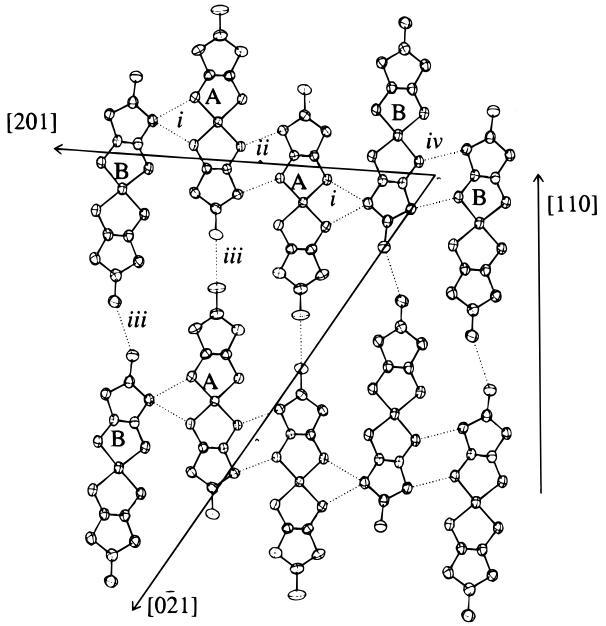

Figure 5. Projection of the $[Ni(dmit)_2]$ layers onto the $(\bar{1}12)$ plane for$[C_1][Ni(dmit)_2]$ (phase **2**). The dotted lines represent the S···S distances shorter than the sum (3.7 Å) of the van der Waals radii.

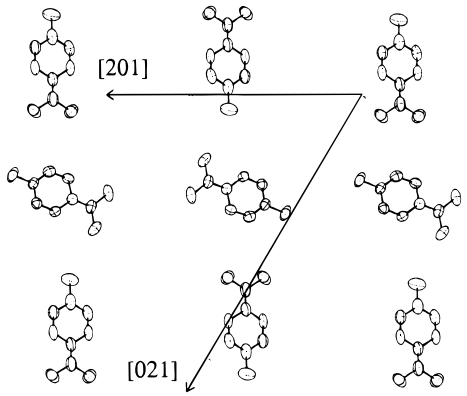

Figure 6. Projection of the centrosymmetric $[C_1]^+$ layers onto the $(\bar{1}12)$ plane for $[C_1][Ni(dmit)_2]$ (phase **2**). H atoms are omitted for clarity.

$[Ni(dmit)_2]^-$ anion is planar (largest deviation 0.062 Å for S(5)). A projection of the structure onto the *bc* plane is shown in Figure 8. The structure consists on alternating chains of $[Ni(dmit)_2]^-$ anions and $[C_2]^+$ cations. The anionic chains, which run along the [100] direction, are built of diades of $[Ni(dmit)_2]^-$ (interplanar distance 3.561 Å) (Figure 9) linked to each other through S···S contacts (Table 3). The angle between the [100] direction

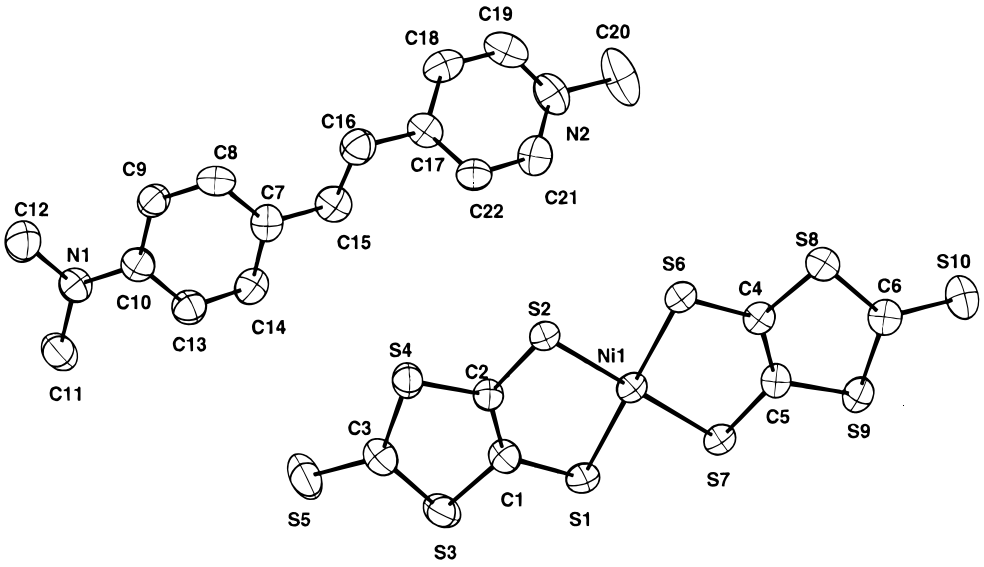

Figure 7. Asymmetric unit and atomic labeling system for $[C_2][Ni(dmit)_2]$ (phase **3**).

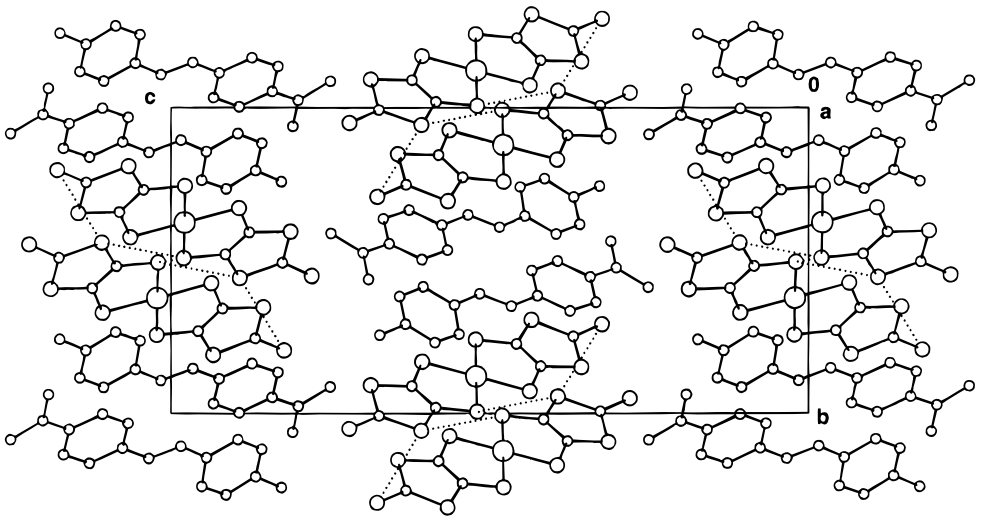

Figure 8. Projection of $[C_2][Ni(dmit)_2]$ unit (phase **3**) onto the *bc* plane.

and the plane of the $[Ni(dmit)_2]$ units is 36.98°. The cations $[C_2]^+$ are not planar: the angle between the two unsaturated rings is 10.54°. Nevertheless, the averaged planes of the $[C_2]^+$ cations are almost parallel to the planes of the $[Ni(dmit)_2]^-$ units (6.27°), but the directions of the longitudinal axis of each molecule form an angle of 6.84°.

$[C_2][Ni(dmit)_2]$ (Phase 4). As for phase **3**, the asymmetric unit contains one $[Ni(dmit)_2]^-$ anion and one $[C2]^+$ cation with the same labeling used in Figure 7. In this compound, the $[Ni(dmit)_2]^-$ units are not as planar as in phase **3**: the largest deviations are 0.165 and 0.140 Å for S(10) and S(5), respectively, indicating a slightly bent structure of the anions. A projection of the structure onto the *ab* plane is shown in Figure 10. The structure is reminiscent of those of $[C_1][Ni(dmit)_2]$ (**1** and **2**) and consists of layers of $[Ni(dmit)_2]^-$ separated by layers of $[C_2]^+$ cations. Contrary to phases **1** and **2**, the anionic layers are built of pairs of $[Ni(dmit)_2]^-$ (interplanar distance 3.65 Å) linked to each others through short S···S contacts (Table 3). Transverse S···S contacts between neighboring molecules are present along the [001] direction (Figure 11) and along the [110] direction, the latter ones involving the external thione groups (Figure 10). The $[C_2]^+$ cations lie between these layers and are arranged in a perpendicular way with respect to the plane of the $[Ni(dmit)_2]^-$ units (94.7°). Opposite to the monoclinic phase **3**, the cations are much more planar: the dihedral angle between the two rings is only 3.2° and the largest deviation is only 0.064 Å for C(19). Along the [001] direction, the cations are stacked head-to-head with an interplanar distance of 3.58 Å, but the adjacent stacks are oriented in such a way that the dimethylamino groups are always pointed toward each other (Figure 12).

Conductivity. The conductivities recorded on single crystals or powder samples are gathered in Table 4. $[C_1][Ni(dmit)_2]$ (phase **2**), $[C_2][Ni(dmit)_2]$ (phases **3** and **4**), and $[C_3][Ni(dmit)_2]$ all exhibit modest powder conductivities in the range10^{-6}—10^{-5} S cm^{-1}, as expected for integral oxidation state 1:1 salts, with a tendency for slightly higher conductivity in $[C_2][Ni(dmit)_2]$. Due to small sizes and squared crystal shapes, no measurements on single crystals could be performed for these three phases. By contrast, very few crystals of phase **1** were obtained, which did not allow a conductivity measurement on powder sample. However, due to their elongated shape, four probes of conductivity measurements were possible on a single crystal for this phase. The room-temperature conductivity is rather high, 1.3 $\times$ 10^{-2} S cm^{-1} with an activation energy (E_a) of 0.05 eV, which is surprising for such a 1:1 salt. Indeed, most of the 1:1 salts

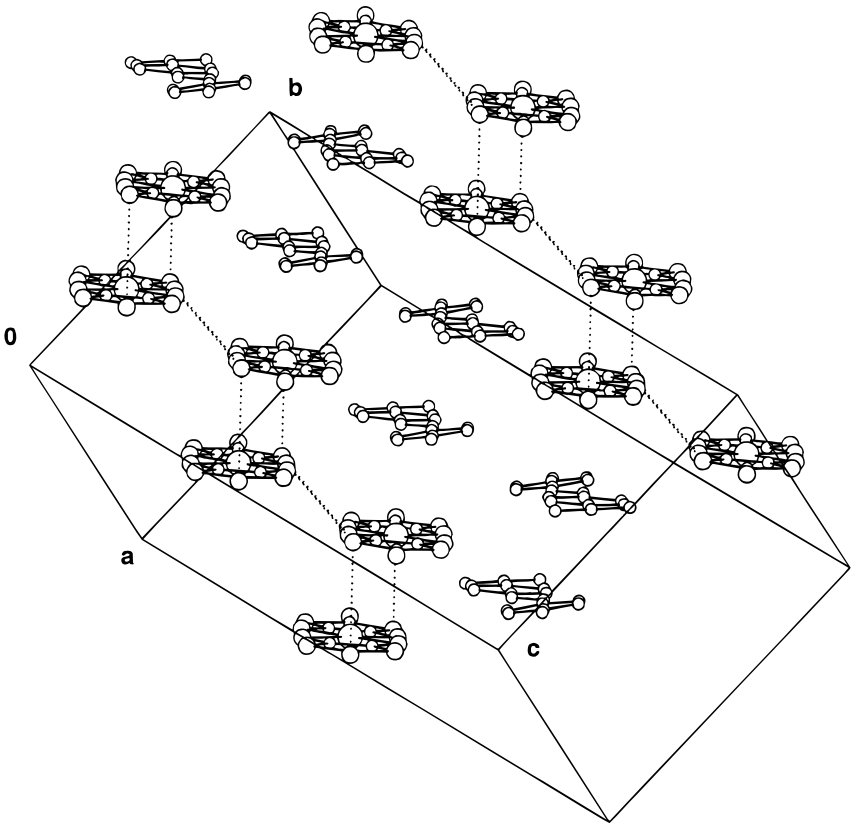

Figure 9. Structure of phase **3** showing the chains of $[Ni(dmit)_2]^-$ along the [100] direction.

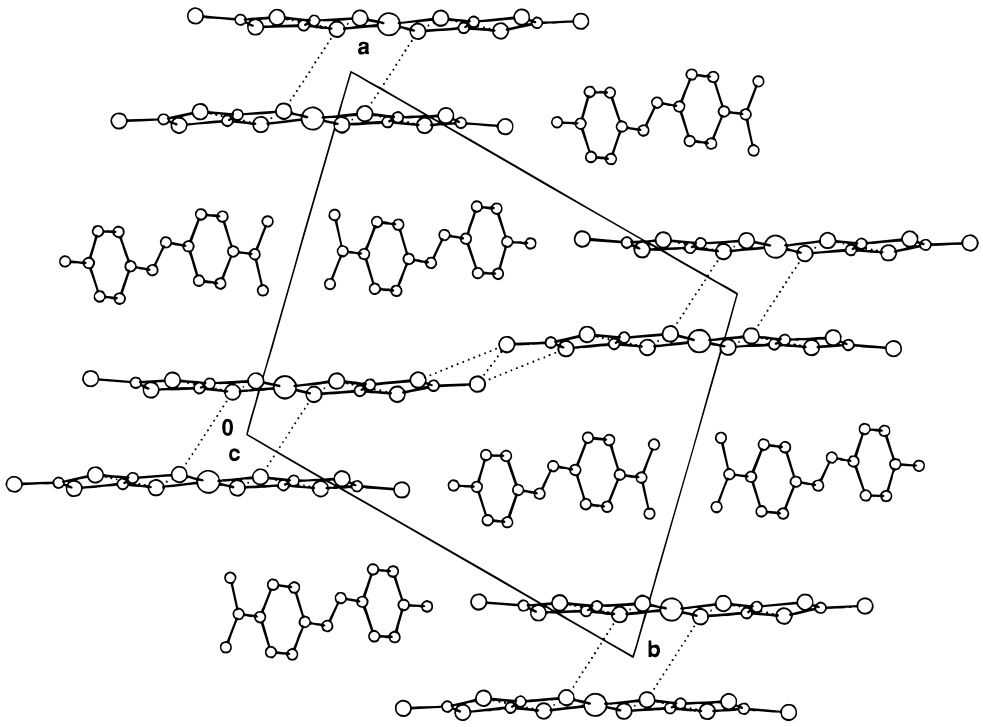

Figure 10. Projection of $[C_2][Ni(dmit)_2]$ unit (phase **4**) onto the *ab* plane.

of $[Ni(dmit)_2]^-$ with closed-shell type cations such as NR_4^+ (R = alkyl), or $SMe_xEt_{3-x}^+$ (x = 1, 2, 3) exhibit conductivities lower than 10^{-5} S cm^{-1}.

The origin of the conductivity is well understood in these systems and depends on short S···S contacts between $[Ni(dmit)_2]^-$ units, the cation being not involved in the electronic properties of the material. The role of the S···S short contacts (Table 3) in the conductivity of phase **1** can be tentatively understood from the examination of the crystal structure. These contacts correspond to a possible interplane path of conductivity. The values of the charge-transfer integrals (β) are gathered in Table 5. The data reveal very small β values in the *ac* plane (Figure 3). While the conductivity in the [001] direction is limited by the weak **B**···**B** interaction (β = 0.0001 eV through (iv)

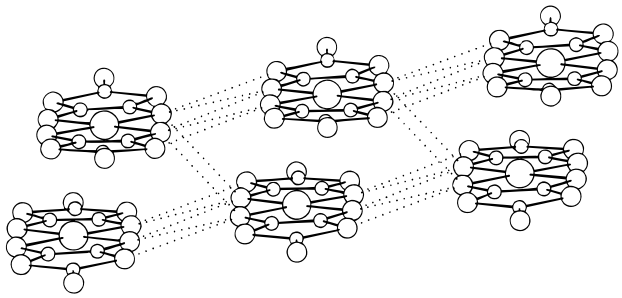

Figure 11. Details of the short S···S contacts along the [001] direction for $[C_2][Ni(dmit)_2]$ (phase **4**).

contacts), the largest interactions are calculated along the [100] direction but are still very modest. This can be qualitatively understood as the result of a π overlap of π orbitals. More interestingly, although no short distances are present along the [010] direction, they correspond to nearly parallel orientations of the molecular units, therefore to σ overlaps of π orbitals associated with large β value (0.1662 eV for **A···B** through v contact). Thus, two paths of conduction can be considered in the *bc* plane along the [021] and [0$\bar{2}$1] directions, both involving **B···A** (v) **A···A** (ii) **A···B** (v) **B···A** (i) interactions and avoiding the weakest **B···B** (iv) interaction.

A similar investigation conducted on phase **2** reveals the same general trend for modest β values in the ($\bar{1}$12) plane even if short S···S are present. As observed in phase **1**, the possibility of large σ overlap along the [$\bar{1}$12] direction allow two paths of conduction in the *ac* plane along the [100] and [001] directions. Phase **3** exhibits a strong one-dimensionnal character, with a conductivity likely dominated by the weak (i) interaction (β = 0.0177 eV) along the [100] direction, while phase **4** exhibits several S···S short contacts in the (1$\bar{1}$0) plane (Figures 10 and 11), all of them being associated with modest β values.

In the above discussion, the cations were assumed to play no role in the conducting properties. Actually, cations with delocalized π system such as 1,2,3-trimethylimidazolium were investigated first by Reedijk et al. with the hope of changing the overall electronic structure through possible π overlap between cations and anions.[25] Such an effect would be expected not only to enhance the conductivity, but also to increase the molecular hyperpolarizability of the NLO chromophore, as previously reported.[27] Although no charge transfer is observed between cations and anions, it is interesting to note that several short distances are observed in the crystal structures (Table 6), although their possible role in the conduction mechanism is not clear. In conclusion, the overall examination of Table 5 indicates transfer integrals lying in the same range of magnitude for every phase investigated in the present study, in agreement with the crystal structures which exhibit the same general features.

Multiproperty [Ni(dmit)$_2$]-Based Materials Exhibiting Second-Order Optical Nonlinearity. A great deal of work has been devoted to the study of compounds derived from M(dmit)$_2$ complexes, with the aim of extending the range of molecular conductors and superconductors based on transition-metal complexes.[10] More recently, metal−bis(dithiolene) was combined with paramagnetic metallocenium counterions,[28−30] with the aim of preparing ferromagnetically ordered molecular-based charge-transfer salts.[31−33] To the best of our knowledge, the present work is the first attempt of combining [Ni(dmit)$_2$] with cationic cyanine dyes, which have emerged as promising candidates for second-order optical nonlinearities.[5,34] However, one of the main bottlenecks to the development of such materials is the compulsory noncentrosymmetric environment of the chromophores if the molecular hyperpolarizability (β) is to contribute to an observable bulk nonlinear susceptibility (χ^2).[35] Various strategies have been reported for the engineering of molecules into noncentrosymmetric arrangements, but the most traditional approach, which guarantees stable noncentrosym-

Table 4. Conductivities (S cm^{-1}) for $[C_1][Ni(dmit)_2]$, $[C_2][Ni(dmit)_2]$, and $[C_3][Ni(dmit)_2]$

		conductivity	
compound	phase	powder	crystal
$[C_1][Ni(dmit)_2]$	**1**		1.3×10^{-2}
	2	10^{-6}	
$[C_2][Ni(dmit)_2]$	**3**	10^{-6} to 10^{-5}	
	4	10^{-6} to 10^{-5}	
$[C_3][Ni(dmit)_2]$		10^{-5}	

Table 5. Transfer Integrals (eV) Calculated with the Partially Filled $[Ni(dmit)_2]^-$ Orbital (Orbital 48) in Several Directions for $[C_1][Ni(dmit)_2]$ (Phases **1** and **2**) and $[C_2][Ni(dmit)_2]$ (Phases **3** and **4**)

phase	direction	contact	symmetry operation[a]	β
1	*ac* plane			
	[100]	**A···A**	iii	0.0051
		B···B	iii	0.0047
	[001]	**A···A**	ii	0.0068
		A···B	i	0.0081
		B···B	iv	0.0001
	bc plane			
	[010]	**B···A**	v[b]	0.1662
2	($\bar{1}$12) plane			
	[110]	**A···A**	iii	0.0017
		B···B	iii	0.0051
	[201]	**A···A**	ii	0.0002
	ac plane			
	[$\bar{1}$12]	**A···A**	v[b]	0.2688
		B···B	v[b]	0.1281
3	[100]		i	0.0177
			ii	0.2214
4	*ab* plane			
			i	0.0059
			ii	0.0375
			iii	0.0019
			iv	0.0035
			v[c]	0.0360

[a] Symmetry operations are labeled according to Table 3. [b] Symmetry operations for second molecule $1 - x$, $^1/_2 + y$, $^1/_2 - z$ (v). [c] Symmetry operation for second molecule $2 - x$, $2 - y$, $1 - z$ (v).

(27) Di Bella, S.; Ratner, M. A.; Marks, T. J. *J. Am. Chem. Soc.* **1992**, *114*, 5842.
(28) Miller, J. S.; Calabrese, J. C.; Epstein, A. J. *Inorg. Chem.* **1989**, *28*, 4230.
(29) Broderick, W. E.; Thompson, J. A.; Godfrey, M. R.; Sabat, M.; Hoffman, B. M. *J. Am. Chem. Soc.* **1989**, *111*, 7656.
(30) (a) Matsubayashi, G.; Yokozawa, A. *Inorg. Chim. Acta* **1992**, *193*, 137. (b) Tanaka, S.; Matsubayashi, G. *J. Chem. Soc., Dalton Trans.* **1992**, 2837. (c) Matsubayasi, G.; Yokozawa, A. *J. Chem. Soc., Dalton Trans.* **1990**, 3535.
(31) Broderick, W. E.; Thompson, J. A.; Day, E. P.; Hoffman, B. M. *Science* **1990**, *249*, 401.
(32) (a) Miller, J. S.; Epstein, A. J. *Angew. Chem., Int. Ed. Engl.* **1994**, *33*, 385. (b) *Chem. Eng. News* **1995**, *73*, 30.
(33) Proceedings of the Conference on Molecular-Based Magnets. *Mol. Cryst. Liq. Cryst.* **1995**, *271*.
(34) (a) Marder, S. R.; Perry, J. W.; Yakymyshyn, C. P. *Chem. Mater.* **1994**, *6*, 1137. (b) Marder, S. R.; Perry J. W.; Schaefer, W. P. *J. Mater. Chem.* **1992**, *2*, 985; (c) Marder, S. R.; Perry J. W.; Schaefer, W. P. *Science* **1989**, *245*, 626.
(35) Williams, D. J. *Angew. Chem., Int. Ed. Engl.* **1984**, *23*, 690.

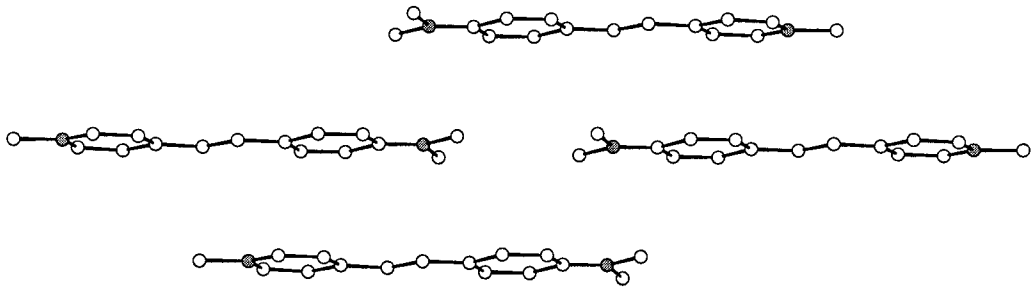

Figure 12. Projection of $[C_2]^+$ layers onto the $(1\bar{1}0)$ plane for $[C_2][Ni(dmit)_2]$ (phase **4**), showing the stacking of cations along the *a* direction.

Table 6. Short Intermolecular Distances (<3.6 Å) between Cations and Anions (in Å) for $[C_1][Ni(dmit)_2]$ (Phases **1** and **2**) and $[C_2][Ni(dmit)_2]$ (Phases **3** and **4**)

atoms	distances	symmetry operations	atoms	distances	symmetry operations
	Phase **1**			Phase **2**	
S(2)−C(21)	3.598(1)	$1-x, 1-y, -z$	S(3)−C(23)	3.544(1)	$x, 1+y, z$
S(3)−C(26)	3.547(1)	$x, y-1, z$	S(4)−N(4)	3.558(1)	$x, 1+y, z$
S(4)−C(22)	3.563(1)	$x, y-1, z$	S(4)−C(27)	3.527(1)	$x, 1+y, z$
S(5)−C(17)	3.590(1)	$1-x, 1-y, -z$	S(10)−C(24)	3.473(1)	x, y, z
S(5)−C(20)	3.546(1)	$1-x, y-{}^1/_2, -z+{}^1/_2$	S(19)−N(3)	3.569(1)	x, y, z
S(8)−C(15)	3.583(1)	$x, y-1, z$	S(16)−C(21)	3.562(1)	x, y, z
S(9)−C(13)	3.573(1)	$x, y-1, z$			
C(21)−S(12)	3.541(1)	$1-x, y+{}^1/_2, -z+{}^1/_2$			
C(25)−S(17)	3.581(1)	$x, 1+y, z$			
C(27)−S(11)	3.562(1)	$1-x, y+{}^1/_2, -z+{}^1/_2$			
S(19)−N(2)	3.575(1)	$1-x, y-{}^1/_2, -z+{}^1/_2$			
	Phase **3**			Phase **4**	
S(7)−C(21)	3.572(1)	$-x, -y, 1-z$	S(6)−C(11)	3.564(1)	$x, 1+y, 1+z$
S(9)−C(22)	3.538(1)	$-x, -y, 1-z$			

metric organizations of NLO chromophores in the solid state, is based on the possibility of growing large noncentrosymmetric single crystals with a high phase-matchable coefficient.[36] A promising approach for reaching this goal, first explored by Meredith,[37] involves the use of cationic chromophores combined with various counteranion. This author observed that most salts of $[C_2]^+$ are noncentrosymmetric. Among them $[C_2]^+[CH_3OSO_3]^+$ exhibited the highest second-order nonlinearity reported at that time.[35] It is now well established that variation of counteranions in these stilbazolium salts is a simple and successful approach for engineering a variety of crystalline materials with large macroscopic optical nonlinearities.[34] Unfortunatly, none of the compounds reported in this paper crystalized in noncentrosymmetric space group. Indeed, a statistical search conducted on every reported structure containing $[Ni(dmit)_2]$ reveals that only two structures in about one hundred entries actually are noncentrosymmetric.

It is interesting to relate the layered structures of $[C_1][Ni(dmit)_2]$ and $[C_2][Ni(dmit)_2]$ to those of the same cations intercalated into $[M_2P_2S_6]$ ($M = Mn^{2+}$, Cd^{2+}). These compounds form a class of lamellar materials made up of $[M]^{2+}$ cations and $[P_2S_6]^{4-}$ anions, which were recently reported as a promising family of magnetic−NLO multiproperty molecular materials.[5] The overall structural features of $[M_2P_2S_6]$- and $[Ni(dmit)_2]$-based structures (phases **1**, **2**, and **4**) bear some ressemblance: they both show lattice of sufur atoms bearing negative charges in which $[C_1]^+$ and $[C_2]^+$ cations are inserted. It was observed that small size pyridinium derivatives (such as $[C_1]^+$) are intercalated with their molecular planes parallel to the sulfur lattices,[38] while C_2^+ and other large chromophores stand edge-on to the slabs of the host $[M_2P_2S_6]$.[5] This trend is observed here also. It can therefore be expected from these similar structural features that two-dimensional $[Ni(dmit)_2]$ materials containing NLO chromophores should offer a promising approach toward multiproperty materials as do $[M_2P_2S_6]$ lamellar compounds.

Further interest arises from the comparison of the physical properties of both family of materials. $[Mn_{1.72}P_2S_6][C_2^+]_{0.56}$ was found to exhibit an efficiency of several hundreds times that of urea in second-harmonic generation.[5] This was tentatively explained by agregation of $[C_2]^+$ species in noncentrosymmetric alignments during the intercalation process into $[Mn_2P_2S_6]$.[39] Without crystal structures, it was not possible to establish unambiguously the origin (kinetic or thermodynamic) of the behavior. Interestingly $[C_1][Ni(dmit)_2]$ (phase **1**) proves the possibility of thermodynamic stability for noncentrosymmetric alignments of cations between guest layers of sulfur atoms. In addition, $[Mn_{1.72}P_2S_6][C_2^+]_{0.56}$ was reported to exhibit permanent magnetization under 40 K even if no interplay was observed between NLO and magnetic properties. $[Ni(dmit)_2]$ is expected to bring the NLO materials with additional conducting properties. The observation of short distances between chromophores and $[Ni(dmit)_2]^-$ species suggests that possible π-overlap between cations and anions could slightly modify of the overall electronic structure and hence the conductivity. Another effect of intermolecular interaction is to modify the molecular hyperpolarizability of the chromophores. This possibility has been thoroughly investigated by Di Bella et al.[24] Therefore this family of hybrid organic−inorganic systems could be promising for engineering multiproperty materials with efficient interplay.

(36) Zyss J.; Oudar, J. L. *Phys. Rev. A* **1982**, *26*, 2028.
(37) Meredith, G. In *Nonlinear Optical Properties of Organic and Polymeric Materials*; Williams, D. J., Ed.; ACS Symposium Series 233; American Chemical Society: Washington, DC, 1983; p 27.
(38) Clément, R.; Lomas, L.; Audière, J. P. *Chem. Mater.* **1990**, *2*, 641.
(39) Coradin, T.; Clément, R.; Lacroix, P. G.; Nakatani, K. *Chem. Mater.* **1996**, *8*, 2153.

Conclusion

This work was part of our general research effort aimed at extending the range of molecular materials combining two properties in the same crystal. We have found that second-order NLO chromophores could be successfully inserted into semiconducting ($\sigma = 10^{-6}$ to 10^{-2} S cm^{-1}) layers of $[Ni(dmit)_2]^-$ anions. Although these materials are found to crystallize in centrosymmetric space group, the crystal structures reveal that acentric layers of chromophores can be stable in some cases. This work is a step in the design of new multiproperty that would theoretically offer potential interest in the emerging optoelectronic technology.

Acknowledgment. R.A. thanks EEC T/raining and Mobility of Researchers Program for a postdoctoral fellowship.

IC971550+